Journal of Organometallic Chemistry 1011 (2024) 123113

Contents lists available at ScienceDirect

Journal of Organometallic Chemistry

journal homepage: www.elsevier.com/locate/jorganchem

Synthesis, structure, and stability of a set of C-stereogenic heteroditopic P, S ligands☆

Aynura Mammadova, Denis Kargin, Clemens Bruhn, Rudolf Pietschnig *

Institute for Chemistry and CINSaT, University of Kassel, Heinrich Plett-Straße 40, 34132 Kassel, Germany

ARTICLE INFO

Keywords:
Phosphorus
Sulfur
Gold (I) complexation
Organolithium
Heteronuclear NMR
Chirality

ABSTRACT

This study focuses on synthesis and investigation of coordination modes of phosphorus and sulfur-containing C-stereogenic compounds, prepared from thioanisole. Isolation of the C-stereogenic organolithium compound $[RR'CHLi{\cdot}2THF]_2$ (R = C_6H_5S, R' = $(CH_3)_3Si$, THF = tetrahydrofuran) instead of *in situ* usage turned out to be mandatory for controlled reactivity. Variation of the steric and electronic properties of the substituents at phosphorus furnished three different phosphane substituted P, S ligands $RR'CHPPh_2$, $RR'CHP(N(C_2H_5)_2)_2$, and $RR'CHP(t\text{-}C_4H_9)_2$. Furthermore, the corresponding chalcogenphosphoranes were synthesized by oxidation with elemental sulfur and selenium. Preliminary investigation of the coordination behavior of $RR'CHP(t\text{-}C_4H_9)_2$, $RR'CHP(S)(t\text{-}C_4H_9)_2$ and $RR'CHP(Se)(t\text{-}C_4H_9)_2$ towards coinage metals was explored with Au(tht)Cl, both for the phosphanes and the corresponding phosphoranes. Intermolecular aurophilic interactions have been observed for the selenophosphorane exclusively.

1. Introduction

In the last few decades the interest in the chemistry of gold (I) has risen rapidly with promising materials being developed for various applications in technology, chemistry, catalysis, and medicine [1–6]. Phosphanes are frequently used as ligands for gold (I) complexes. Current investigations focus on ditopic ligands, which possess two separate donor sites with gradient reactivity for coordination. [7,8] Heteroatoms, such as O, S, N and P in organic molecules carrying one or more lone pairs are used as donor sites in ditopic ligands. Accordingly, sulfur and selenium based chalcogenophosphoranes have been developed progressively due to their applicability in catalysis. [9] Furthermore, using optically active compounds as heteroditopic ligands is of particular interest. [10]

To investigate the coordination behavior of phosphorus and sulfur containing C- stereogenic compounds, a suitable precursor has been prepared. A. Laguna et al. and A. Rodriguez *et al.* described the coordination behavior and metal-metal interactions of coinage metal complexes with heteroditopic ligands such as Ph_2PCH_2SPh. Homo- or heterobimetallic complexes of coinage metals could be obtained by using such an asymmetric bidentate ligand. [1,6] In this contribution, we make use of a similar precursor starting from thioanisole and sequentially introducing a TMS group and thereafter a set of secondary chlorophosphanes, differing in terms of electronic and steric properties (Scheme 1). Moreover, chalcogenophosphoranes of the corresponding ligands were prepared by adopting literature procedures. [11] With a variety of potential ligands in hand, we explored complexation of Au(tht)Cl for selected examples.

2. Results and discussion

2.1. Ligand preparation and properties

As simple starting material silyl compound **2** is accessible from thioanisole **1** by a variety of literature procedures. [12–14] Starting from **2**, *in situ* lithiation and usage of the organolithium compound in the presence of different donors, *e.g.* THF, HMPA, have been reported previously, but spectroscopic data on the isolated organolithium compound are scarce. [14–19] To optimize yield and to reduce the number of by-products, isolation of the organolithium compound **3** turned out to be mandatory. To this end precursor **2** is treated with one equivalent *n*-BuLi in THF at 0 °C. After the reaction a light-yellow solution is obtained. Removing all volatiles *in vacuo* yields a highly viscous oil. Changing the solvent to pentane resulted in precipitation of the product which upon

☆ Dedicated to Professor Dr. Evamarie Hey-Hawkins on the occasion of her retirement

* Corresponding author.
E-mail address: pietschnig@uni-kasel.de (R. Pietschnig).

https://doi.org/10.1016/j.jorganchem.2024.123113
Received 27 February 2024; Received in revised form 22 March 2024; Accepted 24 March 2024
Available online 30 March 2024

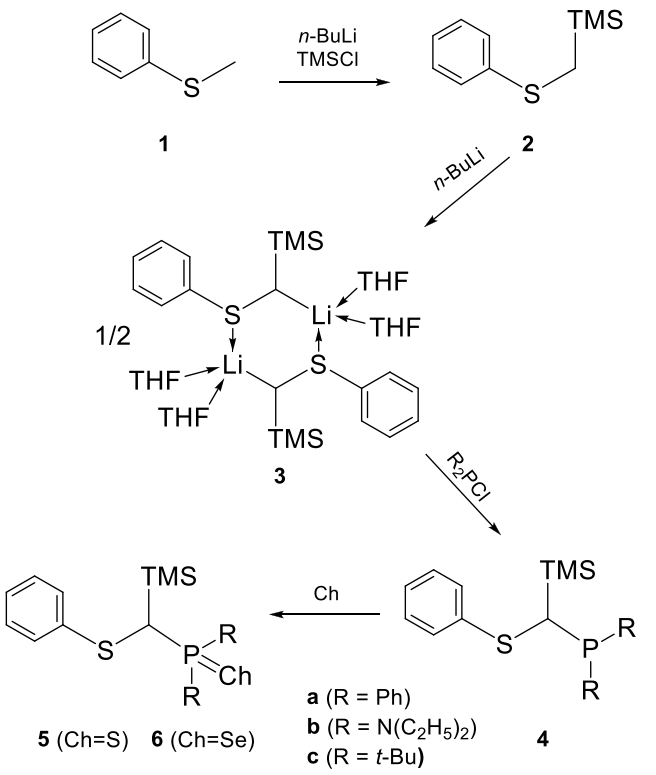

Scheme 1. Schematic outline of the ligand preparation.

recrystallization yields **3** as colorless, amorphous air and moisture sensitive solid. Within the ^{1}H and ^{13}C NMR-spectra of compound **3** recorded in THF-d_8 solution, non-deuterated THF is observed as well. Integration of the amount of coordinated THF is hampered by the overlap of the deuterated and non-deuterated THF signals and possible exchange reactions. To solve this problem, the measurement is repeated in deuterated acetonitrile (CD_3CN) and toluene (toluene-d_8) for better signal separation. ^{1}H NMR of **2** displays a singlet for the two protons of the methylene group at δ = 2.05 ppm ($CDCl_3$). [20] According to integration and 2D NMR (HSQC) spectra of **3**, the signal at δ = 0.60 ppm (toluene-d_8) belongs to the remaining proton of the CH group. Moreover, multiplet signals of hydrogen atoms of the coordinated THF group are observed at δ = 3.50 ppm ($(CH_2)_2(CH_2)_2O$) and at δ = 1.35 ppm ($(CH_2)_2(CH_2)_2O$). In the ^{29}Si NMR of compound **2** (which was not reported in literature) a single resonance at δ = 1.9 ppm (CD_2Cl_2) for the silicon atom of the TMS group is observed. By contrast, the ^{29}Si NMR spectrum of **3** displays a singlet resonance δ = –5.8 ppm for the TMS group, which is shifted to higher field in comparison with **2**. ^{7}Li NMR spectra confirm compound **3** featuring a singlet resonance at δ = –0.6 ppm in CD_3CN or δ = 2.3 ppm in THF-d_8.

The molecular structure of compound **3** is confirmed by a single crystal X-ray diffraction study. As depicted in Fig. 1, compound **3** forms a centrosymmetric six membered ring dimer in the solid state and each lithium ion is coordinated by one carbon atom, one sulfur atom and 2 THF molecules. The Li1-S1' (2.586(3) Å), C1-Li1 (2.194(3) Å) and Li1-O1 (1.923(3) Å) bond lengths in **3** show no peculiarities and are in a similar range as in their desilylated analogs which have been reported before. [21,22] The distance of the lithium atom to the non-bonded sulfur atom (3.042 Å) is smaller than the sum of the Van der Waals radii (r(Li) = 1.81 Å, r(S) = 1.80 Å), [23] therefore stabilizing intramolecular interactions can be anticipated. The centrosymmetric geometry implies that the C-stereogenic centers have opposite absolute configuration with an overall racemic composition in solid **3**.

Treatment of precursor **3** with secondary chlorophosphanes afforded the targeted compounds. To explore different electronic and steric features of the substituents at phosphorus, chloro-(diphenyl)phosphane,

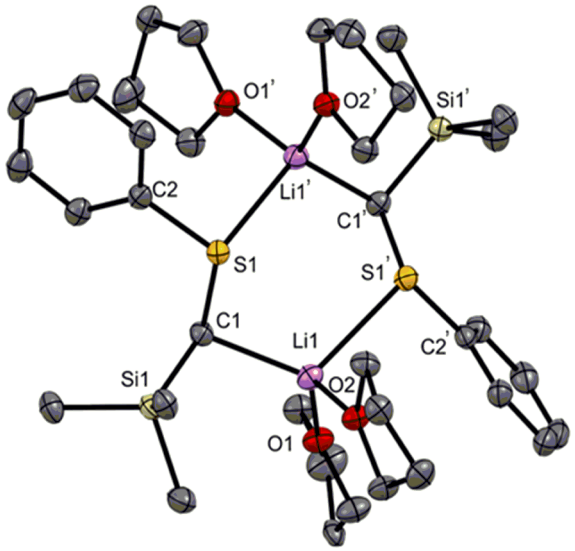

Fig. 1. Ortep plot for the molecular structure of **3** in the solid state with ellipsoids drawn at the 50 % probability level. H atoms are omitted for clarity. Selected bond lengths [Å] and angles [°]: C1-S1 1.7418(15), C2–S1 1.7865(16), S1–Li1' 2.586(3), Li1–C1 2.194(3), S1–C1–Li1' 115.42(8), Si1–C1–Li1 100.61 (9), C1–S1–C2 111.67(7), C2–S1–Li1' 96.98(8).

bis(diethylamino)-chlorophosphane, and chloro-(di-*tert*-butyl)phosphane were chosen as the phosphane components in this work. Steric properties of these substituents can be estimated from their Tolman angle or percent buried volume. According to H. Clavier and S. P. Nolan, (*tert*-Bu)$_3$P shows a higher percent buried volume, followed by P(NMe$_2$)$_3$ and PPh$_3$. [24] For the general procedure, the organolithium compound **3**, suspended in toluene, is treated at room temperature with the above mentioned chlorophosphanes (see Scheme 1). The liquid part of the suspension was separated from LiCl by centrifugation. Subsequent removal of volatile compounds yields compounds **4a-c** as air and moisture-sensitive oily products.

Monitoring the reactions process with ^{31}P NMR spectroscopy, compound **4a** exhibits a signal at δ = –5.4 ppm (90 %), besides tetraphenyldiphosphane at δ = –15.0 ppm (10 %) [25] as a side product. The electron donating phenyl groups at phosphorus lead to a high field shift of the ^{31}P resonance of **4a** compared to compounds **4b** and **4c**. Compound **4b** features a singlet at δ = 87.9 ppm (94 %) being the most deshielded ^{31}P resonance in this series owing to the electronegative diethylamino groups at phosphorus. Compound **4c** was obtained in an isolated yield of ~88 % and does not contain phosphorus-based impurities according to ^{31}P NMR spectra (singlet at δ = 39.9 ppm). The connection between the phosphanyl and the CH group in **4a-c** is confirmed by spin coupling of the phosphorus and the respective hydrogen and carbon nuclei. In the ^{1}H NMR spectra the signal of the CH proton is observed as a doublet with a $^{2}J_{HP}$ coupling of 1–5 Hz resonating at lower field (**4a**: δ ($CDCl_3$) = 3.14 ppm, $^{2}J_{HP}$ = 1.3 Hz; **4b**: δ ($CDCl_3$) = 3.04 ppm, $^{2}J_{HP}$ = 2.5 Hz; **4c**: δ ($CDCl_3$) = 2.71 ppm, $^{2}J_{HP}$ = 5.0 Hz) compared to the starting material **3** (δ (toluene-d_8) = 0.60 ppm). The ^{1}H NMR resonance of the CH group in **4b** was identified with 2D NMR (HSQC spectrum) because of an overlap with the signal for the hydrogen atoms of methylene groups of the diethylamino groups in the 1D spectra. In the ^{13}C NMR spectra, the connectivity of the phosphorus and carbon atoms is corroborated by the respective J_{PC} coupling for the CH group and the carbon atoms of the TMS-group. The ^{29}Si NMR data of these compounds reveal doublets around 5 ppm with up to 28 Hz coupling constant to phosphorus (**4a**: δ = 5.4 ppm, $^{2}J_{SiP}$ = 18 Hz; **4b**: δ = 3.9 ppm, $^{2}J_{SiP}$ = 28 Hz; **4c**: δ = 6.3 ppm, $^{2}J_{SiP}$ = 27 Hz). An overview of the collected NMR data is given in Table 1.

APCI-DIP-HR mass spectrometry confirms the identity of the target compounds displaying the $[M + H]^{+}$ peaks of the protonated molecules.

Table 1
NMR data of compounds **4a; 4b; 4c** (δ in ppm, J in Hz).

Compound	^{1}H NMR		^{13}C NMR		^{29}Si NMR		^{31}P NMR
	δ_{CH}	$^{2}J_{HP}$	δ_{CH}	$^{2}J_{CP}$	δ_{Si}	$^{2}J_{SiP}$	δ_{P}
4a	3.14	1.3	32.4	46	5.4	18	−5.4
4b	3.04	2.5	30.0	41	3.9	28	87.9
4c	2.71	5.0	24.9	69	6.3	27	39.9

As a part of this work, chalcogenophosphoranes of the above-mentioned compounds were prepared by oxidation of the phosphorus atom with elemental chalcogens such as sulfur and red selenium. Oxidation with selenium is advantageous as ^{77}Se-NMR provides additional information of the donor properties of the underlying P(III) unit. As expected, the phosphorus nucleus is deshielded upon oxidation compared to its precursor **4a** (δ = –5.4 ppm). For **5a** the ^{31}P NMR spectrum consists of a singlet at δ = 45.9 ppm. In case of **6a**, within the ^{31}P NMR spectrum the singlet at δ = 38.8 ppm is accompanied by low-intensity satellites with $^{1}J_{PSe}$ = 733 Hz due to coupling of ^{31}P with ^{77}Se. In the complementary ^{77}Se NMR spectrum, a doublet at δ = −324.0 ppm ($^{1}J_{PSe}$ = 729 Hz) for **6a** is observed.

By contrast, aminosubstituted **5b** and **6b** resonate at higher field upon oxidation (**5b**: δ = 78.0 ppm; Δδ = 9.9 ppm; **6b**: δ = 73.3 ppm; Δδ = 14.6 ppm), compared with their precursor **4b** (δ = 87.9 ppm) which may be attributed to the electronic interaction between the P(V) center and the adjacent nitrogen atom. [26] The ^{77}Se satellites in the ^{31}P NMR spectra of **6b** ($^{1}J_{PSe}$ = 769 Hz) match the coupling in the complementary ^{77}Se NMR spectrum, featuring a doublet at δ = −188.4 ppm.

For the *t*Bu substituted phosphoranes the ^{31}P NMR resonances (δ = 83.0 ppm, **5c**; δ = 79.5 ppm, **6c**) are significantly deshielded compared with the corresponding phosphane **4c** (δ = 39.9 ppm). The value of the $^{1}J_{PSe}$ coupling constant (682 Hz) of **6c** is smaller compared to **6a, 6b**, and literature known compound *t*Bu$_2$P(Se)C(S)SR [27] while the chemical shift (δ(^{77}Se) = −306.7 ppm) is in between **6a** and **6b**. The lowest $^{1}J_{PSe}$ value for **6c** suggests the highest basicity of the corresponding phosphane **4c** in this series. [28,29]. ^{77}Se NMR data for compounds **6(a-c)** and *t*Bu$_2$P(Se)C(S)SR [27] are given in Table 2.

The IR spectra of compounds **5a-c** show stretching frequencies for the P=S units as strong bands at 692 cm^{-1} (**5a**), 690 cm^{-1} (**5b**), 661 cm^{-1} (**5c**), respectively, which is similar to previously reported thiophosphoranes. [26,30-31] Additionally, the identity of chalcogenophosphoranes **5a-c** and **6a-c** is confirmed by APCI-DIP-HR mass spectrometry. Furthermore, elemental analyses are in good agreement with the assigned composition. Structural evidence for these chalcogenophosphoranes was obtained from single crystal X-ray crystallography (see ESI files, **Figure S68, Tables S2-S4**). Compounds **5a** and **6a** crystallize in the monoclinic space group P2$_1$/c. Compounds **5b** and **6b** crystallize in the monoclinic space group P2$_1$ as a racemic mixture of *R*− and *S*− enantiomers both being present in the asymmetric unit. The solid-state structures of compounds **5c** and **6c** are depicted in Fig. 2. The latter compounds crystallize in triclinic space group P$\bar{1}$.

The C1-P1 (1.858(3) Å), C1-S2 (1.834(3) Å) bond lengths in **5c** are slightly longer than in compound **5a** (C1-P1: 1.818(4) Å, C1-S2: 1.831 (4) Å). The distance between P1 and S1 in **5c** (1.9622(12) Å) is longer than in **5a** but nearly identical with the literature value of *t*Bu$_2$P(S)C(S)SR. [27] (**5a**: 1.9502(15) Å, *t*Bu$_2$P(S)C(S)SR [27]: 1.964(6) Å). The S2-C1-P1 angle in **5c** (114.35(16)°) is bigger compared to the angle in compounds **5a** and **5b** (**5a**: 108.9(2)°, **5b** *R*: 110.7(2°), **5b** *S*: 106.3(3)°). As expected, the phosphorus atom is pseudo-tetrahedrally surrounded (sum of angles: 327°) in line with reported *t*Bu$_2$P(S)C(S)SR (sum of angles: 325°). [27] The C1-P1 (1.860(5) Å), C1-S1 (1.846(5) Å) distances in **6c** are longer than in **6a** (C1-P1: 1.825(2) Å, C1-S1: 1.836(2) Å). The bulky tert-butyl groups slightly increase the P=Se (2.1301(14) Å) bond length in **6c** compared to compounds **6a, 6b** and *t*Bu$_2$P(Se)C(S)SR. [27] (**6a**: 2.1041(7) Å, **6b**: (2.101(5) Å, *t*Bu$_2$P(Se)C(S)SR [27]: 2.1172(8) Å). Additionally, the P1-C1-S1 (113.5(3)°) angle in **6c** is larger in comparison with bond angles of compounds **6a** and **6b** (**6a**: 108.94(12)°, **6b**: 107.2(9)°)), but in line with reported complex [Au$_2$(PPh$_2$CH$_2$SPh)$_2$](CF$_3$SO$_3$)$_2$ (116.9(2)) [1].

Table 2
^{77}Se NMR data for compounds **6(a-c)** and tBu$_2$P(Se)C(S)SR (δ in ppm, J in Hz).

Compound	^{77}Se NMR	
	δ_{Se}	$^{1}J_{SeP}$
6a	−324.0	729
6b	−188.4	769
6c	−306.7	683
*t*Bu$_2$P(Se)C(S)SR [27]	−384.4	711

A closer look at the solid state structures of the oxidized compounds **5a-c** shown in Fig. 3 reveals information on the arrangement of the donor atoms, most likely related to the steric situation of the substituents at phosphorus (as all selenium based compounds are isostructural to the sulfur based ones, only the latter will be discussed). In the molecular structures the orientation of the TMS and phenylsulfanyl group are slightly different but could become meaningful regarding complexation reactions. In **5a** and **5c** the sulfur atoms S1 and S2 point in the similar direction, while in **5c** the sulfur atoms point in opposite directions. Owing to the sterically demanding *tert*-butyl groups at phosphorus, the TMS group is forced in a position pointing towards S1. Hindered rotation around the P-C1 bond may be assumed and taking this into account the S1-S2 distances and torsion angles are useful descriptors. The distance between the phosphorus bound S1 atom and the S2 atom of the phenylsulfanyl unit in **5a** is nearly identical compared with **5b**, but substantially shorter than the distance in compound **5c** (**5a**: 3.688 Å; **5b**: 3.645 Å; **5c**: 4.728 Å). The torsion angle (∠S1PC1S2) in **5c** is significantly larger than the related torsion angles in compounds **5a** and **5b** (**5a**: 64.88°; **5b**: 68.54°; **5c**: 152.07°). Complementary, the ∠S1PC1Si torsion angle is almost indistinguishable in compounds **5a** and **5b**, but smaller in **5c** (**5a**: 53.09°; **5b**: 51.73°; **5c**: 15.34°). The coordination capability of S2 could be strongly dependent on these geometrical features and may be considered as a promising aspect for future investigations of complexation behavior of **5a** and **5b**. The position of the S2 atom enables intramolecular coordination in a chelating fashion along with S1 to a metal center. By contrast, in **5c** intermolecular coordination of the S2 atom along with S1 of a second molecule to form linear strands seems more feasible.

2.2. Complexation towards Au(tht)Cl

To explore the ligand properties of the ditopic C-stereogenic compounds, complexation reactions were carried out with Au(I). The corresponding Au(I) complexes can be synthesized via treatment of Au(tht)Cl with an equimolar amount of ligand in toluene and are diamagnetic which enables NMR spectroscopic analysis. According to Rodriguez *et al.* and LAGUNA *et al.*, [6] the reaction of a heteroditopic P, S ligand such as **4c** with Au(tht)Cl enables selective coordination of the phosphorus atom to the metal center, replacing tetrahydrothiophene Scheme 2.

Although, the purity of the starting material was ensured, the ^{31}P NMR spectrum of the crude reaction mixture displays two signals at lower field with chemical shifts values at δ = 71.3 ppm as the main product (94%) and δ = 70.2 ppm (6%) as a side product compared to the resonance of the free ligand **4c** (δ = 39.9 ppm). Upon recrystallization, both products were isolated. The identities of complexes **7c** (main product) and its desilylated analog **7c'** (side product) is confirmed independently by APCI-DIP-HR and APCI-DIP mass spectrometry with peaks corresponding to dehalogenated molecular ion [M-Cl]$^{+}$. Furthermore, elemental analysis confirms the purity of target complex **7c** after recrystallisation. Coordination of the phosphorus atom to the gold atom leads according to the ^{1}H NMR spectrum to deshielding of the CH proton with an increase of the coupling constant to the phosphorus atom in **7c** compared to the free ligand **4c** (**4c**: δ = 2.71 ppm, $^{2}J_{HP}$ = 5.0

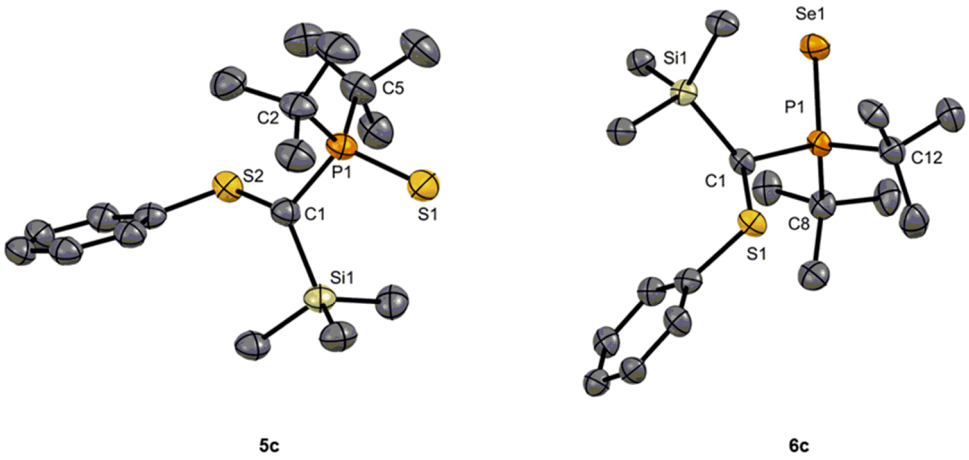

Fig. 2. Ortep plots for the molecular structure of **5c** in the solid state (left) and **6c** (right) ellipsoids drawn at the 50 % probability level. H atoms are omitted for clarity. In **5c**, the phenylsulfanyl group is disordered in a 1:9 ratio. The molecule with 90 % probability is depicted. Hydrogen atoms have been omitted for clarity. Selected bond lengths [Å] and angles [°]: **(5c)** P1-S1 1.9622(12), P1-C1 1.858(3), P1-C2 1.873(4), P1-C5 1.877(4), C1-Si1 1.929(3), C1-S2 1.834(3), C1-P1-C2 104.75 (15), C1-P1-C5 110.17(16), C2-P1-C5 112.10(17). **(6c)** P1-Se1 2.1301(14), P1-C1 1.860(5), P1-C8 1.883(5), P1-C12 1.896(6), C1-Si1 1.927(5), C1-S1 1.846(5), C1-P1-C8 104.9(2), C1-P1-C12 110.5(2) C8-P1-C12 112.4(2).

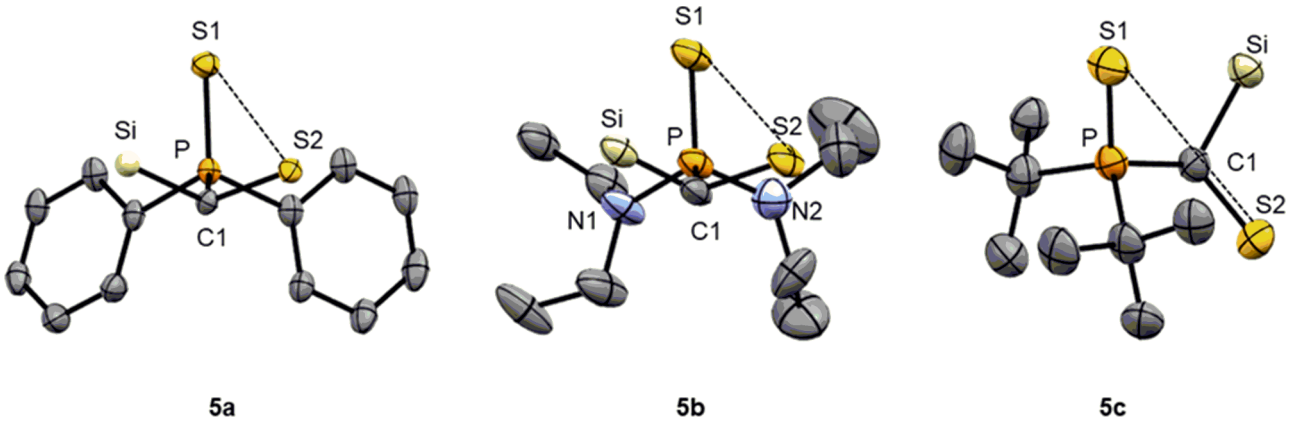

Fig. 3. Comparison of the molecular structure of compounds **5a, 5b** and **5c**. Hydrogen atoms, phenyl groups from phenylsulfanyl moieties and methyl groups from TMS have been omitted for clarity.

Hz; **7c**: δ = 3.10 ppm, $^{2}J_{HP}$ = 15.2 Hz). As it seems, gold coordination of **4c** facilitates protodesilylation of the backbone possibly owing to the presence of chloride or traces of water. Nevertheless, desilylation occurs only in minor amount consistent with the latter explanation.

To gain insight into the coordination motif of **7c** suitable crystals were studied with single crystal X-ray diffraction. The molecular structure is depicted in Fig. 4. The asymmetric unit of **7c** contains half of the molecule, which is completed by symmetry operations defined by the space group (P21/m). The phenylsulfanyl group and proton of CH group are disordered over two positions (50 %), only one position is found in the asymmetric unit. The X-ray structure reveals a linear geometry at the gold atom with a P-Au-Cl angle of 179.33(6)° for **7c**, which is expected for gold(I) complexes. [32] Evidence for the steric and electronic influence of the TMS group can be seen in the slight elongation of the P1-C1 bond lengths of **7c** (1.860(7)Å) slightly differing from the side product (**7c'**: 1.835(5)Å) and literature known complex $[Au_2(PPh_2CH_2SPh)_2](CF_3SO_3)_2$ (1.831 (4)) [1]. The P1-Au1 distances are identical in both complexes (**7c**: 2.2452 (16)Å, **7c':** 2.2487(12) Å) and in good agreement with the literature value of the triarylphosphane derivative [AuCl(PPh_3)], in which the Au-P distance is 2.235 (3) Å. [33] For the sulfur atom in complex **7c** being 4.884 Å away from the gold in the solid state structure, bonding interactions with the gold atom can be ruled out.

Further investigation of the coordination motifs with gold was performed starting from thiophosphorane ligand **5c**. Following the same procedure as described in literature, the reaction with Au(tht)Cl leads to formation of the target complex **8c**. Changes of the chemical environment in NMR spectroscopic investigations are tiny compared to the changes observed in the formation of **7c**. After the reaction, the ^{31}P NMR spectrum of **8c** exhibits a sharp singlet shifted only 1.9 ppm to lower field (δ = 84.9 ppm) compared with the resonance of the free ligand **5c** (δ = 83.0 ppm). In the ^{1}H NMR spectrum, the characteristic CH proton in **8c** is deshielded with an almost identical coupling constant to the phosphorus atom (**8c**: δ = 3.69 ppm, $^{2}J_{HP}$ = 19.3 Hz; **5c:** δ = 3.31 ppm, $^{2}J_{HP}$ = 17.6 Hz). In the crude reaction mixture, a minor by-product is observed in *ca.* 2 % amount which would be consistent with a hypothetic desilylated **8c'** (not depicted). However, we have not been able to isolate this by-product to firmly establish its identity.

The identity of complex **8c** is confirmed by ESI-HR mass spectrometry with an isotope pattern corresponding to the ion ([M-Cl]$^{+}$ at *m/z* 569.1191 100 %). Additionally, the elemental analysis confirms the purity of complex **8c** after recrystallisation. According to single crystal X-ray diffraction of Au(I) complex **8c** in the solid state, the sulfur atom adjacent to phosphorus coordinates the metal center. The molecular structure of **8c** is shown in Fig. 5. Complex **8c** crystallizes in the orthorhombic, chiral space group Iba2. The *S*-enantiomer with the Flack parameter of −0.017(13) can be assigned, refined with an R value of 4 %. The S1-P1-C1 102.6(4)°) bond angle in **8c** decreases upon

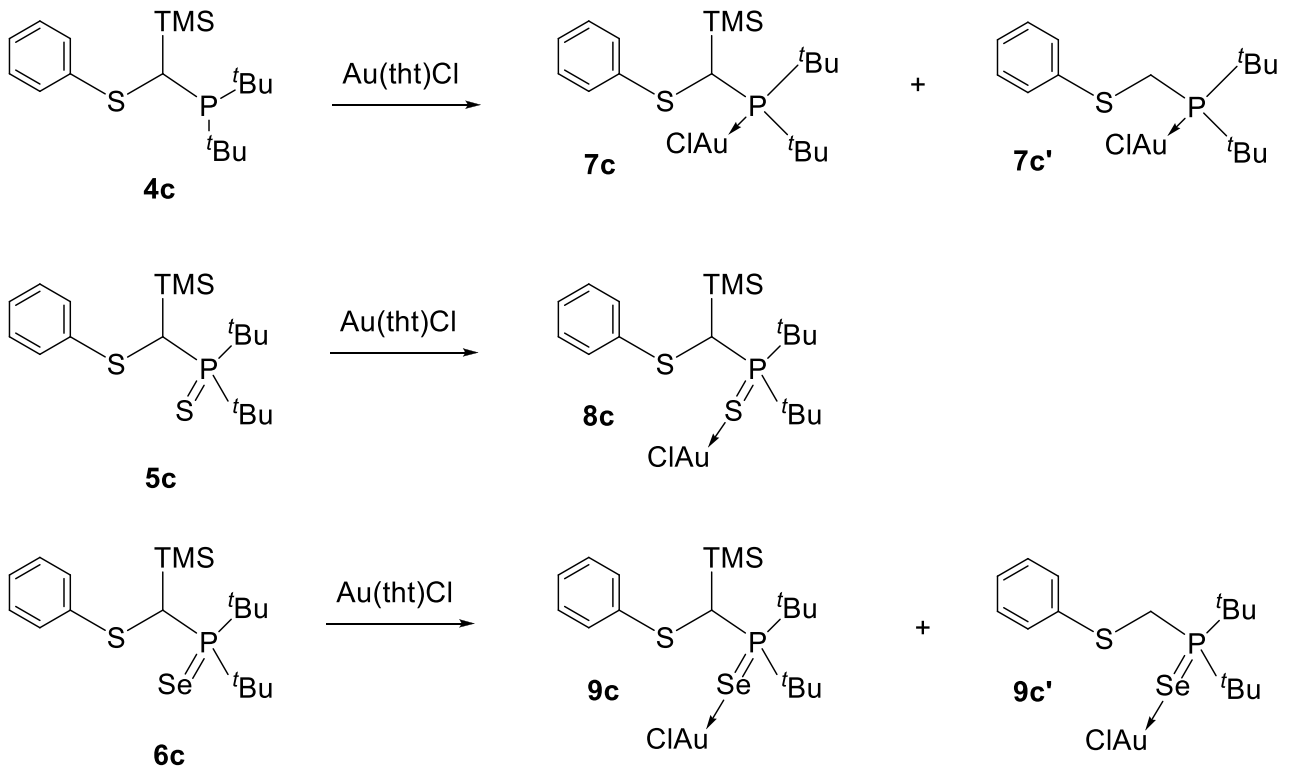

Scheme 2. Reaction scheme for the synthesis of the Au (I) complexes.

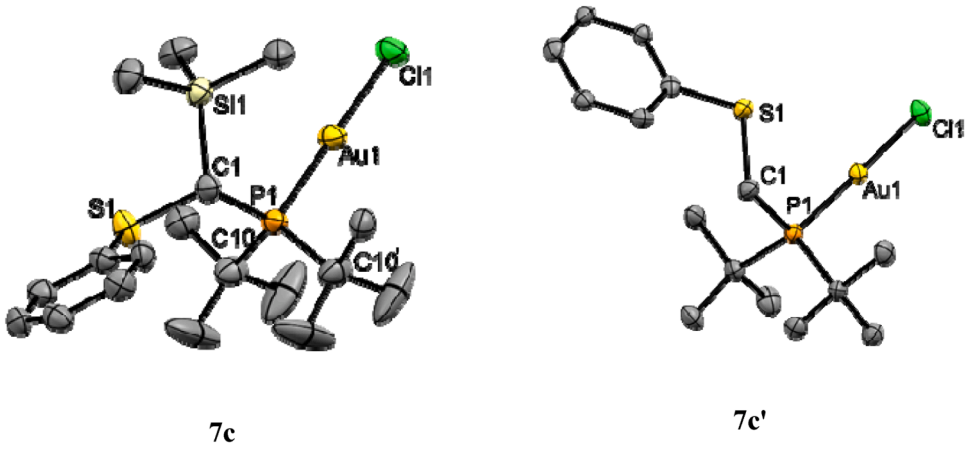

Fig. 4. Ortep representation of the molecular structure of Au (I) complexes **7c** (left) and **7c'** (right). Hydrogen atoms have been omitted for clarity. Thermal ellipsoids are drawn at the 50 % probability level. Selected bond lengths [Å] and angles [°]: **(7c)** P1-C1 1.860(7), P1-Au1 2.2452(16), Au1-Cl1 2.2871(16), C1-S1 1.801(5), C1-Si1 1.921(7), C10-P1-C10' 114.4(3), C1-P1-C10 107.7(2), C1-P1-C10' 107.7(2), S1-C1-P1 116.4(3), P1-C1-Si1 117.8(3), P1-Au1-Cl1 179.33(6). **(7c')** P1-C1 1.835(5), P1-Au1 2.2487(12), Au1-Cl1 2.3048(12), C1-S1 1.814(5), S1-C1-P1 110.5(3), P1-Au1-Cl1 177.53(4), C1-P1-Au1 112.85(17).

coordination (**5c:** (109.48(11)°). The sum of angles at the phosphorus atom in complex **8c** (333°) is slightly larger compared to the sum of angles in starting material **5c** (327°) with phosphorus adopting a tetrahedral geometry as well. Additionally, the molecular geometry of sulfur is bent with a bond angle of 108.70(15)° (P1-S1-Au1). In the IR spectra of complex **8c**, the P=S stretching vibration is observed as a medium strong band at 610 cm^{-1} whereas the free ligand **5c** shows a strong band at 661 cm^{-1}. Upon coordination, the P=S stretching vibration changes accordingly to lower wavenumbers indicating a weakening of the P=S bond by gold coordination, consistent with a variety of compounds in literature. [26]

Finally, for selenophosphorane ligand **6c** coordination of Au(I) was explored as well. The reaction with Au(tht)Cl leads to formation of the targeted complex **9c**. After the reaction, the ^{31}P NMR spectrum of **9c** exhibits a sharp singlet shifted only 0.7 ppm to higher field (δ = 78.8 ppm) compared with the free ligand **6c** (δ = 79.5 ppm). In the ^{1}H NMR spectrum, the characteristic CH proton in **9c** is deshielded with an almost identical coupling to the phosphorus nucleus (**9c**: δ = 3.98 ppm, $^{2}J_{HP}$ = 19.1 Hz; **6c:** δ = 3.37 ppm, $^{2}J_{HP}$ = 17.0 Hz). The ^{77}Se satellites in the ^{31}P NMR spectra of **9c** ($^{1}J_{PSe}$ = 518 Hz) match the coupling in the complementary ^{77}Se NMR spectrum, featuring a doublet at δ = −186.7 ppm. Upon complexation, the value of the $^{1}J_{PSe}$ coupling constant of **9c** is decreased compared with the free ligand **6c** (683 Hz).

The molecular structure of the **9c** has been studied with single crystal X-ray diffraction and is depicted in Fig. 6. As in the case of gold complex **7c**, where a desilylated by-product had been observed, for **9c** a similar

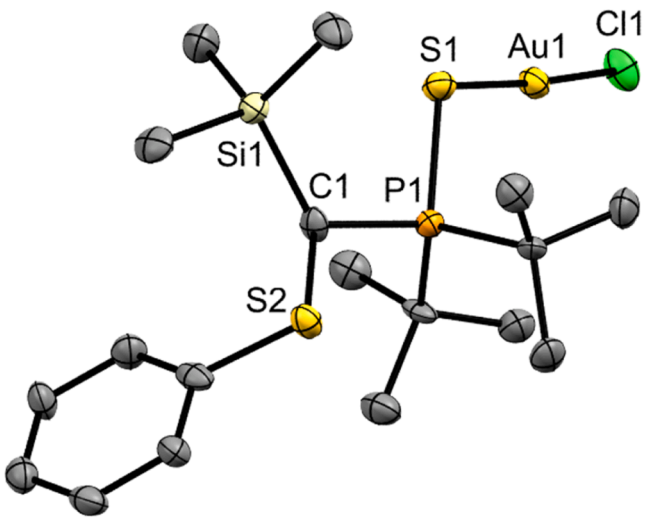

Fig. 5. Ortep representation of the molecular structure of complex **8c**. Hydrogen atoms have been omitted for clarity. Thermal ellipsoids are drawn at the 50 % probability level. Selected bond lengths [Å] and angles [°]: P1-C1 1.837(11), S1- P1 2.038(4), Au1-S1 2.269(3), Au1-Cl1 2.275(3), S1-Au1-Cl1 175.41(11), P1-S1-Au1 108.70(15), C1-P1-S1 102.6(4), S2-C1-P1 112.3(6).

desilylated analog **9c'** has been observed as a trace (3 %). Although the amount of **9c'** was insufficient for full characterization a single crystal suitable for X-ray diffraction has been measured and the structure refined (See **Figure S69**). Complex **9c** crystallizes in the monoclinic space group $P2_1/c$. The asymmetric unit of compound **9c** contains one molecule and the second molecule is generated by symmetry operation. Upon complexation the P-Se distance in ligand **5c** (2.1301(14) Å) undergoes a slight elongation in **9c** (2.2042(18) Å) which hardly changes by protodesilylation as observed in **9c'** (2.1919(10) Å). The X-ray structure reveals a linear geometry at the gold atom with an Se1-Au1-Cl1 angle of 172.29(4)° for **9c**, which is in good agreement with the desilylated by-product **9c'** (175.87(3)°). Additionally, the bond angle P1-Se1-Au1 (100.09(5)°) in **9c** is consistent with **9c'** (103.21(3)°). Remarkably, out of all obtained gold(I) complexes in this study, only **9c** shows intermolecular aurophilic interactions with an Au···Au distance of 3.1597(13) Å (Fig. 6) which is in the usual range for such interactions in literature. [34]

3. Conclusions

In summary, we have explored a range of novel C-stereogenic heteroditopic P, S ligands and their coordination behavior was investigated through complexation reactions with Au(tht)Cl. To obtain suitable precursors, an efficient synthetic route for preparation of compounds **4a-c** was developed. Isolation of C-stereogenic compound **3** starting from **2** turned out to be mandatory and led in subsequent reactions to compounds **4a-c** in high yield and acceptable purity. Changing the substitution pattern at the phosphorus atom with regard to electronic and steric features provides a set of ligands for complexation reactions. For this purpose, compounds **4a-c** were synthesized in salt metathesis reactions of compound **3** with various phosphane-halogenides. Preparation of more stable phosphane chalcogenides (**5a-c** and **6a-c**) starting from compounds **4a-c** was investigated. The corresponding phosphane chalcogenides (**5a-c** and **6a-c**) were prepared by adapted procedures using elemental sulfur and selenium. Having a variety of possible compounds suitable for coordination to gold, the coordination behavior of phosphorus and sulfur-containing C-stereogenic ligands was investigated. The most promising results were obtained starting from *tert*-butyl substituted phosphane **4c** and **5c** as crystallization could be used as a work-up procedure. Employing ligand **4c** in a reaction with Au(tht)Cl, novel phosphorus only coordinated gold(I) complexes (**7c**) could be prepared and characterized. Oxidizing the phosphorus atom with sulfur and selenium prevented the phosphorus lone pair from coordination. The introduced chalcogen atom was capable of coordinating the gold atom and compounds **8c** and **9c** were obtained from chalcogenophosphoranes **5c** and **6c** with Au(tht)Cl. On some instances desilylated complexes **7c'** and **9c'** were obtained as a side product during the complexation reaction, in which the stereogenic nature of the carbon atom adjacent to phosphorus is lost. All complexes were structurally characterized by single crystal X-ray diffraction. Remarkably, selenophosphorane complex **9c** is the only complex in our series featuring aurophilic interactions. Given the racemic nature of lithiated **3**, the resulting ligands are racemic as well. In future work we will explore the possibility for chiral induction in the metalation step to get access to chiral versions of the here presented ligands.

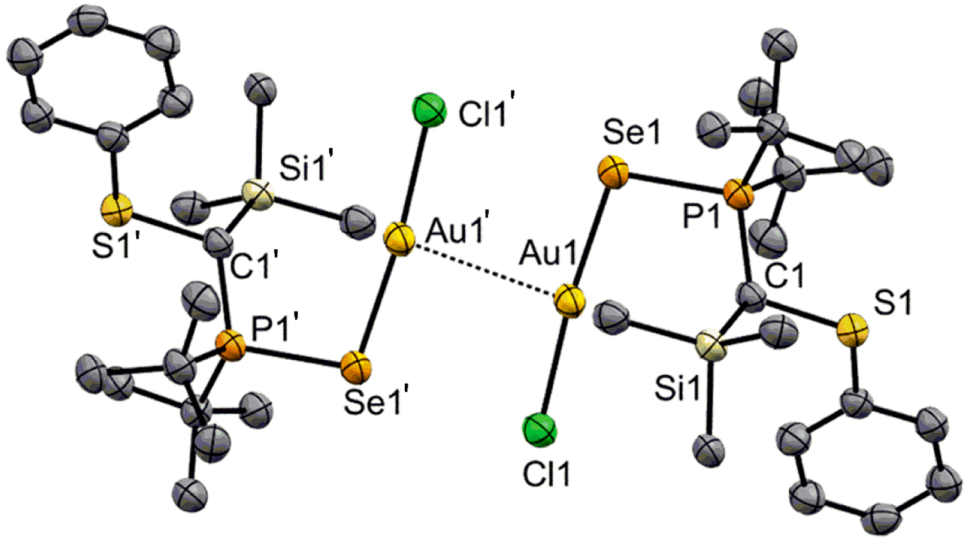

Fig. 6. Ortep representation of the molecular structure of complex **9c**. Hydrogen atoms have been omitted for clarity. Thermal ellipsoids are drawn at the 50 % probability level. Selected bond lengths [Å] and angles [°]:P1-C1 1.839(6), Se1- P1 2.2042(18), Au1-Se1 2.3832(8), Au1-Cl1 2.2882(16), Au1-Au1' 3.1597(13), Se1-Au1-Cl1 172.29(4), P1-Se1-Au1 100.09(5), C1-P1-Se1 108.6(2), S1-C1-P1 113.6(3).

4. Experimental details

4.1. General procedures

All manipulations with air or moisture-sensitive substances were performed in an argon atmosphere (Argon 5.0) under exclusion of moisture (drying column with P_5O_{10}) and oxygen or in a conventional glovebox. Before being used, the glassware was dried in an oven at 120 °C. Solvents were freshly distilled over drying agents, prescribed in CRC Handbook of chemistry and subsequently stored under argon atmosphere over 4 Å molecular sieves. The NMR solvents were purchased from Deutero GmbH and finally stored over 3 Å molecular sieves under argon atmosphere. Commercially available reagents and chemicals ($PhSCH_3$; Ph_2PCl; $(t\text{-}Bu)_2PCl$; DABCO; Au(tht)Cl; elemental sulfur; red selenium) were purchased from commercial suppliers and used as received. $((C_2H_5)_2N)_2PCl$ was synthesized according to literature procedures. [35] Compound **2** was synthesized according to a literature procedure. [13] All NMR spectra were recorded on Jeol JNM-ECZL500, Varian 500 VNMRS and Varian MR-400 spectrometers at 22 °C. Chemical shifts (δ) were expressed in parts per million [ppm] with respect to the following standards, set as 0 ppm: $SiMe_4$ (for ^1H and ^{13}C, ^{29}Si) and 85 % phosphoric acid (for ^{31}P) and Me_2Se (for ^{77}Se). Coupling constants (*J*) are given in Hertz (Hz). Multiplicities of signals are described as follows: *s* = singlet, *d* = doublet, *m* = multiplet. Electrospray ionization (ESI) and APCI-DIP (atmospheric pressure chemical ionization-direct inlet probe) mass determinations were performed on a Finnigan LCQ Deca (ThermoQuest) using samples dissolved in HPLC-quality tetrahydrofuran. Elemental analyses were performed with a HEKAtech Euro EA CHNS elemental analyzer (Wegberg, Germany). Samples were prepared in a Sn cup and analyzed with added V_2O_5. Results were verified by double determination. Any solvent in crystalline material (**3**) was verified by NMR analysis and the expected values for elemental analyses were calculated accordingly. IR spectra were recorded on a Bruker Alpha II ECO-ATR spectrometer and analyzed with Opus 8.2.28 (32 bits) of Bruker Optics. X-ray diffraction experiments were performed by using either a STOE IPDS 2 [image plate (diameter 34 cm) using Mo-GENIX source (λ = 0.71073 Å)] or a STOE StadiVari [using either Mo-GENIX source (λ = 0.71073 Å), or Cu-GENIX source (λ = 1.54186 Å)] diffractometer. Structures were solved using dual space method (SHELXT) and were refined with SHELXL-2018. [36] Evaluation of the data sets and graphical preparation of the structures were carried out using Olex2 [37] and Mercury [38]. Details of the structure determination and refinement are summarized in **Tables S1–S7** (supporting information). Data on the structures reported here had been deposited with the Cambridge Crystallographic Data Center. CCDC 2335326 – 2335336 and 2342024 contain the supplementary crystallographic data for this paper. These data can be obtained free of charge via www.ccdc.cam.ac.uk/data_request/cif, or by emailing data_request@ccdc.cam.ac.uk, or by contacting The Cambridge Crystallographic Data Centre, 12 Union Road, Cambridge CB2 1EZ, UK; fax: +44 1223 336033.

5. Synthetic protocols and characterization

5.1. Synthesis of 3

3.2 g (16.2 mmol) of 1-(phenylsulfanyl)-1-trimethylsilyl-methane **2** were dissolved in 20 mL dry THF and cooled to 0 °C. While stirring at 0 °C, 6.8 mL (16.9 mmol, 2.5 M) n-BuLi solution in hexane were added dropwise according to an adopted literature procedure. The reaction mixture was stirred at 0 °C for another 1 h giving a light-yellow solution. All volatile compounds were removed *in vacuo* yielding a highly viscous oil. Upon addition of pentane, a colorless solid precipitated which was washed with pentane (3 × 10 mL) and centrifuged. The collected pentane phases were stored separately. After being dried under reduced pressure, 4.8 g (13.9 mmol, 86 %) compound **3** was obtained as a colorless solid. Colorless crystalline material suitable for X-ray diffraction analysis was obtained after recrystallization from pentane.

^1H NMR (400 MHz, toluene-d_8) δ [ppm]: 6.91–7.56 (m, 5H, C_{ar}); 3.50 (m, 4H, $(CH_2)_2(CH_2)_2O$); 0.60 (s, 1H, C*H*); 1.35 (m, 4H, $(CH_2)_2(CH_2)_2O$); 0.33 (s, 9H, TMS).^{13}C NMR (101 MHz, toluene-d_8) δ [ppm]: 152.3 (s, *ipso-C*, C_{ar}); 127.9 (s, *ortho-C*, C_{ar}); 124.8 (s, *meta-C*, C_{ar}); 123.1 (s, *para-C,* C_{ar}); 68.4 (s, $(CH_2)_2(CH_2)_2O$); 25.5 (s, $(CH_2)_2(CH_2)_2O$); 3.3 (s, *C*H); 3.2 (s, TMS). ^7Li NMR (194 MHz, THF-d_8) δ [ppm]: 2.3 (s). ^7Li NMR (194 MHz, CD_3CN) δ [ppm]: −0.6 (s). ^{29}Si NMR (99 MHz, THF-d_8) δ [ppm]: −5.8 (s). Elemental analysis (%): calculated for $C_{18}H_{31}LiO_2SSi$: C 62.39, H 9.02, S 9.25, found: C 62.25, H 9.10, S 8.76.

5.2. Synthesis of 4a

1.33 g (3.84 mmol) of **3** were dissolved in 20 mL dry toluene. 0.85 g (3.84 mmol) chlorodiphenylphosphane was added dropwise to a stirred solution at room temperature. The reaction was allowed to proceed for an hour, resulting in a suspension with bright yellow liquid phase and colorless precipitate which was removed via centrifugation and washed two more times with 20 mL pentane. The organic phase was combined, and all volatiles were removed *in vacuo*. 1.04 g of compound **4a** (2.7 mmol, 71 %) were obtained as a yellow oil. The product was 90 % pure by NMR spectroscopy. The compound was used without further purification in the next step.

^1H NMR (500 MHz, $CDCl_3$) δ [ppm]: 7.10–7.72 (m, 15H, C_{ar}); 3.14 (d, $^2J_{HP}$ = 1.3 Hz, C*H*); − 0.04 (s, 9H, TMS).^{13}C NMR (101 MHz, $CDCl_3$) δ [ppm]: 126.0–138.8 (m, C_{ar}); 32.4 (d, $^1J_{CP}$ = 46 Hz, *C*H); −0.8 (d, $^3J_{CP}$ = 5 Hz, TMS). ^{29}Si NMR (99 MHz, $CDCl_3$) δ [ppm]: 5.4 (d, $^2J_{SiP}$ = 18 Hz). ^{31}P NMR (202 MHz, $CDCl_3$) δ [ppm]: − 5.4 (s). MS (APCI-DIP-HR) *m/z* = 381.1256 ($[M + H]^+$ 58 %), calculated: 381.1262.

5.3. Synthesis of 4b

0.970 g (2.8 mmol) of compound **3** were dissolved in 20 mL dry toluene. 0.589 g (0.6 mL, 2.8 mmol) bisdiethylaminochlorophosphane were added dropwise to a stirred solution at room temperature. The reaction was allowed to proceed for an hour, resulting in a suspension with bright yellow liquid phase and colorless precipitate which was removed via centrifugation and washed two more times with 20 mL pentane. The organic phases were combined, and all volatiles were removed *in vacuo*. 0.718 g of compound **4b** (1.9 mmol, 69 %) were obtained as a yellow oil. The product was 96 % pure by NMR spectroscopy. The compound was used without further purification in the next step.

^1H NMR (500 MHz, $CDCl_3$) δ [ppm]: 7.08–7.34 (m, 5H, C_{ar}); 3.06 (m, 4H, $N(CH_2CH_3)_2$); 3.04 (d, $^2J_{HP}$ = 2.5 Hz, C*H*); 2.95 (m, 4H, $N(CH_2CH_3)_2$); 1.07 (m, 6H, $N(CH_2CH_3)_2$); 0.97 (m, 6H, $N(CH_2CH_3)_2$); 0.11 (s, 9H, TMS). ^{13}C NMR (101 MHz, $CDCl_3$) δ [ppm]: 139.7 (d, $^3J_{CP}$ = 5 Hz, *ipso-C*, C_{ar}); 128.6 (s, *ortho-C*, C_{ar}); 128.1 (d, $^4J_{CP}$ = 2 Hz, *meta-C*, C_{ar}); 124.9 (s, *para-C,* C_{ar}); 43.3 (d, $^2J_{CP}$ = 18 Hz, $N(CH_2CH_3)_2$); 42.9 (d, $^2J_{CP}$ = 16 Hz, $N(CH_2CH_3)_2$); 30.0 (d, $^1J_{CP}$ = 41 Hz, *C*H); 14.5 (d, $^3J_{CP}$ = 3 Hz, $N(CH_2CH_3)_2$); 14.3 (d, $^3J_{CP}$ = 4 Hz, $N(CH_2CH_3)_2$); −0.4 (d, $^3J_{CP}$ = 6 Hz, TMS). ^{29}Si NMR (99 MHz, $CDCl_3$) δ [ppm]: 3.9 (d, $^2J_{SiP}$ = 28 Hz). $^{31}P\{^1H\}$ NMR (202 MHz, $CDCl_3$) δ [ppm]: 87.9 (s). MS (APCI-DIP-HR) *m/z* = 371.2100 ($[M + H]^+$ 100 %), calculated: 371.2106

5.4. Synthesis of 4c

1.00 g (2.88 mmol) of **3** were dissolved in 20 mL dry toluene. 0.52 g (2.88 mmol) bis-*tert*-butyl-chloro-phosphane were added dropwise to a stirred solution at room temperature. The workup followed as above. 0.86 g of compound **4c** (2.5 mmol, 88 %) were obtained as yellow oil. The product was 98 % pure by NMR spectroscopy. ^1H NMR (500 MHz, $CDCl_3$) δ [ppm]: 7.11–7.31 (m, 5H, C_{ar}); 2.71 (d, $^2J_{HP}$ = 5.0 Hz, C*H*); 1.38 (d, $^3J_{HP}$ = 11.9 Hz, 9H, $C(CH_3)_3$); 1.23 (d, $^3J_{HP}$ = 11.2 Hz, 9H, $C(CH_3)_3$); 0.12 (s, 9H, TMS). ^{13}C NMR (101 MHz, $CDCl_3$) δ [ppm]: 139.8

(d, $^{3}J_{CP}$ = 2 Hz, *ipso-C*, C_{ar}); 128.9 (s, *ortho-C*, C_{ar}); 127.9 (s, *meta-C*, C_{ar}); 125.3 (s, *para-C,* C_{ar}); 34.1 (d, $^{1}J_{CP}$ = 16 Hz, $C(CH_3)_3$); 33.8 (d, $^{1}J_{CP}$ = 15 Hz, $C(CH_3)_3$); 32.0 (d, $^{2}J_{CP}$ = 14 Hz, $C(CH_3)_3$); 30.3 (d, $^{2}J_{CP}$ = 14 Hz, $C(CH_3)_3$); 24.9 (d, $^{1}J_{CP}$ = 69 Hz, *CH*); 0.3 (d, $^{3}J_{CP}$ = 7 Hz, TMS). ^{29}Si NMR (99 MHz, $CDCl_3$) δ [ppm]: 6.3 (d, $^{2}J_{SiP}$ = 27 Hz). ^{31}P {^{1}H} NMR (202 MHz, $CDCl_3$) δ [ppm]: 39.9 (s). MS (APCI-DIP-HR) *m/z* = 341.1882 ([*M* + *H*]$^{+}$ 3.4 %), calculated: 341.1888.

5.5. Sulfur derivatives 5a-c

A Schlenk-flask charged with a suspension of elemental sulfur (for **4a**: 0.017 g, 0.525 mmol; for **4b**: 0.017 g, 0.540 mmol; for **4c**: 0.019 g, 0.587 mmol) and **4a-c** (**a**: 0.2 g, 0.525 mmol; **b**: 0.2 g, 0.540 mmol; **c**: 0.2 g, 0.587 mmol) in pentane (20 mL) was sonicated for an hour at room temperature, resulting in a cloudy solution. After filtration and removal of all the volatiles, analytically pure product was crystallized from suitable solvent (pentane or DCM) at ambient temperature.

(5a). Yield: 83 %. ^{1}H NMR (500 MHz, $CDCl_3$) δ [ppm]: 6.91–7.94 (m, 15H, C_{ar}); 3.54 (d, $^{2}J_{HP}$ = 10.7 Hz, C*H*); 0.19 (d, $^{4}J_{HP}$ = 1.4 Hz, TMS); ^{13}C NMR (101 MHz, $CDCl_3$) δ [ppm]: ^{13}C NMR (101 MHz, $CDCl_3$) δ [ppm]: 126.7–137.3 (m, C_{ar}); 37.9 (d, $^{1}J_{CP}$ = 36 Hz, *CH*); −0.2 (d, $^{3}J_{CP}$ =2 Hz, TMS). ^{29}Si NMR (99 MHz, $CDCl_3$) δ [ppm]: 5.9 (d, $^{2}J_{SiP}$ = 4 Hz). ^{31}P{^{1}H} NMR (202 MHz, $CDCl_3$) δ [ppm]: 45.9 (s). MS (APCI-DIP-HR) *m/z* = 413.0977 ([*M* + *H*]$^{+}$ 86 %), calculated: 413.0882. Elemental analysis (%): calculated for $C_{22}H_{25}PS_2Si$: C 64.04, H 6.11, S 15.54, found: C 64.01, H 6.14, S 15.41. IR (ATR) 689 cm^{-1} (s, *P=S*).

(5b). Yield: 75 %. ^{1}H NMR (400 MHz, $CDCl_3$) δ [ppm]: 7.12–7.25 (m, 5H, C_{ar}); 3.29 (d, $^{2}J_{HP}$ = 16.8 Hz, C*H*); 3.05 (m, 8H, $2N(CH_2CH_3)_2$); 1.05 (m, 12H, $2N(CH_2CH_3)_2$); 0.31 (s, 9H, TMS). ^{13}C NMR (101 MHz, $CDCl_3$) δ [ppm]: 138.4 (s, *ipso-C*, C_{ar}); 129.1 (s, *ortho-C*, C_{ar}); 127.6 (s, *meta-C*, C_{ar}); 125.9 (s, *para-C,* C_{ar}); 41.0 (d, $^{2}J_{CP}$ = 4 Hz, $N(CH_2CH_3)_2$); 39.9 (d, $^{2}J_{CP}$ = 4 Hz, $N(CH_2CH_3)_2$); 36.3 (d, $^{1}J_{CP}$ = 69 Hz, *CH*); 14.4 (d, $^{3}J_{CP}$ = 2 Hz, $N(CH_2CH_3)_2$); 13.7 (d, $^{3}J_{CP}$ = 3 Hz, $N(CH_2CH_3)_2$); 0.7 (d, $^{3}J_{CP}$ =2 Hz, TMS). ^{29}Si NMR (99 MHz, $CDCl_3$) δ [ppm]: 5.2 (d, $^{2}J_{SiP}$ = 5 Hz). ^{31}P {^{1}H} NMR (202 MHz, $CDCl_3$) δ [ppm]: 78.0 (s). MS (APCI-DIP-HR) *m/z* = 403.1821 ([*M* + *H*]$^{+}$ 4.18 %), calculated: 403.1826. Elemental analysis (%): calculated for $C_{18}H_{35}N_2PS_2Si$: N 6.96, C 53.69, H 8.76, S 15.92, found: N 7.19, C 53.34, H 8.88, S 15.91. IR (ATR) 690 cm^{-1} (s, *P=S*).

(5c). Yield: 70 %. ^{1}H NMR (500 MHz, $CDCl_3$) δ [ppm]: 7.19–7.34 (m, 5H, C_{ar}); 3.31 (d, $^{2}J_{HP}$ = 17.6 Hz, C*H*); 1.57 (d, $^{3}J_{HP}$ = 15.8 Hz, 9H, $C(CH_3)_3$); 1.37 (d, $^{3}J_{HP}$ = 15 Hz, 9H, $C(CH_3)_3$); 0.41 (d, $^{4}J_{HP}$ = 1.0 Hz, 9H, TMS). ^{13}C NMR (101 MHz, $CDCl_3$) δ [ppm]: 138.1 (d, $^{3}J_{CP}$ = 2 Hz, *ipso-C*, C_{ar}); 129.3 (s, *ortho-C*, C_{ar}); 126.2 (s, *meta-C*, C_{ar}); 125.6 (s, *para-C,* C_{ar}); 40.7 (d, $^{1}J_{CP}$ = 17 Hz, $C(CH_3)_3$); 40.3 (d, $^{1}J_{CP}$ = 20 Hz, $C(CH_3)_3$); 29.5 (d, $^{2}J_{CP}$ = 1 Hz, $C(CH_3)_3$); 29.2 (d, $^{1}J_{CP}$ =15 Hz, *CH*); 27.9 (d, $^{2}J_{CP}$ = 1 Hz, $C(CH_3)_3$); 2.4 (d, $^{3}J_{CP}$ =2 Hz, TMS). ^{29}Si NMR (99 MHz, $CDCl_3$) δ [ppm]: 8.5 (d, $^{2}J_{SiP}$ = 2 Hz). ^{31}P {^{1}H} NMR (202 MHz, $CDCl_3$) δ [ppm]: 83.0 (s). MS (APCI-DIP-HR) *m/z* = 373.1603 ([*M* + *H*]$^{+}$ 70.3 %), calculated: 373.1608. Elemental analysis (%): calculated for $C_{18}H_{33}PS_2Si$: C 58.02, H 8.93, S 17.21, found: C 58.05, H 8.81, S 17.44. IR (ATR) 661cm^{-1} (s, *P=S*).

5.6. Selenium derivatives 6a-c

A Schlenk-flask charged with a suspension of red selenium (for **4a**: 0.021 g, 0.262 mmol; for **4b**: 0.051 g, 0.646 mmol; for **4c**: 0.046 g, 0.587 mmol) and **4 (a-c)** (**a**: 0.1 g, 0.262 mmol; **b**: 0.2 g, 0.539 mmol; **c**: 0.2 g, 0.587 mmol) in pentane (20 mL) was sonicated for an hour at room temperature. During this time the suspension turns dark. After filtration and removal of all the volatiles, analytically pure compound was crystallized from suitable solvent (pentane or DCM) pentane at ambient temperature.

(6a). Yield: 88 %. ^{1}H NMR (400 MHz, CD_2Cl_2) δ [ppm]: 6.88–790 (m, 15H, C_{ar}); 3.77 (d, $^{2}J_{HP}$ = 11.7 Hz, C*H*); 0.14 (s, 9H, TMS); ^{13}C NMR (101 MHz, CD_2Cl_2) δ [ppm]: ^{13}C NMR (101 MHz, CD_2Cl_2) δ [ppm]: 127.0–133.2 (m, C_{ar}); 37.2 (d, $^{1}J_{CP}$ = 27 Hz, *CH*); − 0.2 (d, $^{3}J_{CP}$ =2 Hz, TMS). ^{29}Si NMR (99 MHz, $CDCl_3$) δ [ppm]: 6.4 (d, $^{2}J_{SiP}$ = 5 Hz). ^{31}P{^{1}H} NMR (202 MHz, CD_2Cl_2) δ [ppm]: 38.8 (s) (satellites d, $^{1}J_{SeP}$ = 733 Hz); ^{77}Se NMR (95 MHz, $CDCl_3$) δ [ppm]: − 324.0 (d, $^{1}J_{SeP}$ = 729 Hz). MS (APCI-DIP-HR) *m/z* = 461.0422 ([*M* + *H*]$^{+}$ 10.5 %), calculated: 461.0427. Elemental analysis (%): calculated for $C_{22}H_{25}PSSeSi$: C 57.50, H 5.48, S 6.98, found: C 57.62, H 5.51, S 6.63.

(6b). Yield: 71 %. ^{1}H NMR (500 MHz, C_6D_6) δ [ppm]: 6.84–7.16 (m, 5H, C_{ar}); 3.61 (d, $^{2}J_{HP}$ = 17.3 Hz, C*H*); 2.98 (m, 8H, $2N(CH_2CH_3)_2$); 0.98 (m, 12H, $2N(CH_2CH_3)_2$); 0.49 (d, $^{4}J_{HP}$ = 1.0 Hz, 9H, TMS). ^{13}C NMR (101 MHz, C_6D_6) δ [ppm]: 138.8 (d, $^{3}J_{CP}$ = 3 Hz, *ipso-C*, C_{ar}); 129.3 (s, *ortho-C*, C_{ar}); 127.3 (s, *meta-C*, C_{ar}); 125.8 (s, *para-C,* C_{ar}); 41.4 (d, $^{2}J_{CP}$ = 4 Hz, $N(CH_2CH_3)_2$); 40.3 (d, $^{2}J_{CP}$ = 4 Hz, $N(CH_2CH_3)_2$); 38.0 (d, $^{1}J_{CP}$ = 53 Hz, *CH*); 14.2 (d, $^{3}J_{CP}$ = 2 Hz, $N(CH_2CH_3)_2$); 13.3 (d, $^{3}J_{CP}$ = 4 Hz, $N(CH_2CH_3)_2$); 1.4 (d, $^{3}J_{CP}$ = 2 Hz, TMS). ^{29}Si NMR (99 MHz, $CDCl_3$) δ [ppm]: 5.6 (d, $^{2}J_{SiP}$ = 6 Hz). ^{31}P {^{1}H} NMR (202 MHz, C_6D_6) δ [ppm]: 73.3 (s) (satellites d, $^{1}J_{SeP}$ = 769 Hz); ^{77}Se NMR (95 MHz, $CDCl_3$) δ [ppm]: − 188.4 (d, $^{1}J_{SeP}$ = 769 Hz). MS (APCI-DIP-HR) *m/z* = 451.1265 ([*M* + *H*]$^{+}$ 4.13 %), calculated: 451.1271. Elemental analysis (%): calculated for $C_{18}H_{35}N_2PSSeSi$: N 6.23, C 48.09, H 7.85, S 7.13, found: N 6.27, C 48.34, H 7.96, S 6.74.

(6c). Yield: 73 %. ^{1}H NMR (400 MHz, $CDCl_3$) δ [ppm]: 7.19–7.34 (m, 5H, C_{ar}); 3.37 (d, $^{2}J_{HP}$ = 17.0 Hz, C*H*); 1.59 (d, $^{3}J_{HP}$ = 15.7 Hz, 9H, $C(CH_3)_3$); 1.41 (d, $^{3}J_{HP}$ = 15.2 Hz, 9H, $C(CH_3)_3$); 0.45 (s, 9H, TMS). ^{13}C NMR (101 MHz, $CDCl_3$) δ [ppm]: 137.9 (d, $^{3}J_{CP}$ = 1 Hz, *ipso-C*, C_{ar}); 129.3 (s, *ortho-C*, C_{ar}); 126.2 (s, *meta-C*, C_{ar}); 125.7 (s, *para-C,* C_{ar}); 40.5 (d, $^{1}J_{CP}$ = 28 Hz, $C(CH_3)_3$); 39.8 (d, $^{1}J_{CP}$ = 31 Hz, $C(CH_3)_3$); 29.9 (d, $^{2}J_{CP}$ = 2 Hz, $C(CH_3)_3$); 28.7 (d, $^{1}J_{CP}$ = 6 Hz, *CH*); 28.6 (d, $^{2}J_{CP}$ = 2 Hz, $C(CH_3)_3$); 2.8 (d, $^{3}J_{CP}$ =1 Hz TMS). ^{29}Si NMR (99 MHz, $CDCl_3$) δ [ppm]: 9.2 (d, $^{2}J_{SiP}$ = 3 Hz). ^{31}P NMR (202 MHz, $CDCl_3$) δ [ppm]: 79.5 (s) (satellites d, $^{1}J_{SeP}$ = 682 Hz); ^{77}Se NMR (95 MHz, $CDCl_3$) δ [ppm]: − 306.7 (d, $^{1}J_{SeP}$ = 683 Hz). MS (APCI-DIP-HR) *m/z* = 421.1047 ([*M* + *H*]$^{+}$ 17.8 %), calculated: 421.1053. Elemental analysis (%): calculated for $C_{18}H_{33}PSSeSi$: C 51.53, H 7.93, S 7.64, found: C 51.51, H 7.79, S 7.37.

5.7. Gold complexes with 4c-6c

A Young flask was charged with compound **4c** (0.06 g, 0.176 mmol), **5c** (0.04 g, 0.107 mmol), **6c** (0.04 g, 0.095 mmol) and 0.056 g (0.176 mmol), 0.034 g (0.107 mmol) or 0.030 g (0.095 mmol) Au(tht)Cl in 6 ml toluene. The reaction mixture was kept at room temperature for 30 min. All volatiles were removed, crude compound of **7c** were obtained as colorless solid. Crude compound of the **8c, 9c** as a bright yellow oil. Single crystals were grown by slow diffusion of pentane into a solution of toluene or dichloromethane at room temperature.

Gold complex 7c. Yield: 88 %. ^{1}H NMR (500 MHz, CD_2Cl_2) δ [ppm]: 7.20–7.34 (m, 5H, C_{ar}); 3.10 (d, $^{2}J_{HP}$ = 15.2 Hz, C*H*); 1.58 (d, $^{3}J_{HP}$ = 16.8 Hz, 9H, $C(CH_3)_3$); 1.36 (d, $^{3}J_{HP}$ = 16.6 Hz, 9H, $C(CH_3)_3$); 0.47 (d, $^{4}J_{HP}$ = 1.0 Hz, 9H, TMS). ^{13}C NMR (101 MHz, CD_2Cl_2) δ [ppm]: 137.9 (s, *ipso-C*, C_{ar}); 129.9 (s, *ortho-C*, C_{ar}); 127.5 (s, *meta-C*, C_{ar}); 126.7 (s, *para-C,* C_{ar}); 39.3 (d, $^{1}J_{CP}$ = 25 Hz, $C(CH_3)_3$); 38.9 (d, $^{1}J_{CP}$ = 22 Hz, $C(CH_3)_3$); 32.1 (d, $^{2}J_{CP}$ = 6 Hz, $C(CH_3)_3$); 30.6 (d, $^{2}J_{CP}$ = 6 Hz, $C(CH_3)_3$); 30.0 (d, $^{1}J_{CP}$ = 6 Hz, *CH*); 1.5 (d, $^{3}J_{CP}$ = 3 Hz, TMS). ^{29}Si NMR (99 MHz, CD_2Cl_2) δ [ppm]: 8.6 (d, $^{2}J_{SiP}$ = 8 Hz). ^{31}P NMR (202 MHz, CD_2Cl_2) δ [ppm]: 71.3. MS (APCI-DIP-HR) *m/z* = 537.1469 ([M-Cl]$^{+}$ 11 %), calculated: 537.1475. Elemental analysis (%): calculated for $C_{18}H_{33}AuClPSSi$: C 37.73, H 5.81, S 5.60, found: C 37.59, H 5.49, S 5.37.

Gold complex 7c'. ^{1}H NMR (400 MHz, CD_2Cl_2) δ [ppm]: 7.29–7.46 (m, 5H, C_{ar}); 3.34 (d, $^{2}J_{HP}$ = 7.7 Hz, C*H*); 1.41 (d, $^{3}J_{HP}$ = 15.4 Hz, 18H, $2C(CH_3)_3$)). ^{13}C NMR (101 MHz, CD_2Cl_2) δ [ppm]: 136.2 (s, *ipso-C*, C_{ar}); 130.2 (s, *ortho-C*, C_{ar}); 129.6 (s, *meta-C*, C_{ar}); 127.6 (s, *para-C,* C_{ar}); 36.4 (d, $^{1}J_{CP}$ = 25 Hz, $2C(CH_3)_3$); 29.7 (d, $^{2}J_{CP}$ = 5 Hz, $2C(CH_3)_3$); 26.2 (d, $^{1}J_{CP}$ = 23 Hz, *CH*). ^{31}P{^{1}H}NMR (202 MHz, CD_2Cl_2) δ [ppm]: 70.2 (s). MS (APCI-DIP) *m/z* = 465.1184 ([M-Cl]$^{+}$ 100 %), calculated: 465.1080.

Gold complex 8c. Yield: 71 %. ^{1}H NMR (400 MHz, CD_2Cl_2) δ [ppm]: 7.24–7.37 (m, 5H, C_{ar}); 3.69 (d, $^{2}J_{HP}$ = 19.3 Hz, C*H*); 1.61 (d, $^{3}J_{HP}$ =

12.5 Hz, 9H, C(CH_3)$_3$); 1.57 (d, $^3J_{HP}$ = 12.8 Hz, 9H, C(CH_3)$_3$); 0.48 (d, $^4J_{HP}$ = 0.8 Hz, 9H, TMS). ^{13}C NMR (101 MHz, CD_2Cl_2) δ [ppm]: 136.2 (d, $^3J_{CP}$ = 2 Hz, *ipso-C*, C_{ar}); 130.1 (s, *ortho-C*, C_{ar}); 127.0 (s, *meta-C*, C_{ar}); 126.9 (s, *para-C,* C_{ar}); 41.5 (d, $^1J_{CP}$ = 28 Hz, *C*(CH$_3$)$_3$); 40.7 (d, $^1J_{CP}$ = 33 Hz, *C*(CH$_3$)$_3$); 31.5 (d, $^1J_{CP}$ = 11 Hz, CH); 29.7 (d, $^2J_{CP}$ = 1 Hz, C(CH_3)$_3$); 29.6 (s, C(CH_3)$_3$); 2.6 (d, $^3J_{CP}$ =1 Hz, TMS). ^{29}Si NMR (99 MHz, CD_2Cl_2) δ [ppm]: 10.5 (d, $^2J_{SiP}$ = 1 Hz). ^{31}P {^{1}H} NMR (202 MHz, CD_2Cl_2) δ [ppm]: 84.9 (s). MS (ESI-HR) *m/z* = 569.1191 ([M-Cl]$^+$ 100 %), calculated: 569.1172. Elemental analysis (%): calculated for $C_{18}H_{33}AuClPS_2Si$: C 35.73, H 5.50, S 10.60, found: C 35.92, H 5.57, S 10.25. IR (ATR) 610 cm^{-1} (s, *P=S*).

Gold complex 9c. ^{1}H NMR (500 MHz, $CDCl_3$) δ [ppm]: 7.20–7.37 (m, 5H, C_{ar}); 3.98 (d, $^2J_{HP}$ = 19.1 Hz, C*H*); 1.62 (d, $^3J_{HP}$ = 4.3 Hz, 9H, C(CH_3)$_3$); 1.59 (d, $^3J_{HP}$ = 5.0 Hz, 9H, C(CH_3)$_3$); 0.51 (d, $^4J_{HP}$ = 0.9 Hz, 9H, TMS). ^{13}C NMR (101 MHz, CD_2Cl_2) δ [ppm]: 136.2 (s, *ipso-C*, C_{ar}); 130.0 (s, *ortho-C*, C_{ar}); 126.9 (s, *meta-C*, C_{ar}); 126.7 (s, *para-C,* C_{ar}); 41.6 (d, $^1J_{CP}$ = 21 Hz, *C*(CH$_3$)$_3$); 40.5 (d, $^1J_{CP}$ = 26 Hz, *C*(CH$_3$)$_3$); 31.5 (d, $^1J_{CP}$ = 3 Hz, CH); 30.1 (s, 2C(CH_3)$_3$); 2.9 (d, $^3J_{CP}$ = 2 Hz, TMS). ^{29}Si NMR (99 MHz, CD_2Cl_2) δ [ppm]: 10.7 (d, $^2J_{SiP}$ = 2 Hz). ^{31}P{^{1}H}NMR (202 MHz, $CDCl_3$) δ [ppm]: 78.8 (s) (satellites d, $^1J_{SeP}$ = 518 Hz); ^{77}Se NMR (95 MHz, $CDCl_3$) δ [ppm]: − 186.7 (d, $^1J_{SeP}$ = 518 Hz). MS (ESI-HR) *m/z* = 617.0609 ([M-Cl]$^+$ 100 %), calculated: 617.0635. Elemental analysis (%): calculated for $C_{18}H_{33}AuClPSSeSi$: C 33.16, H 5.10, S 4.92, found: C 34.30, H 4.98, S 4.43.

CRediT authorship contribution statement

Aynura Mammadova: Writing – original draft, Investigation, Data curation. **Denis Kargin:** Validation, Data curation. **Clemens Bruhn:** Resources. **Rudolf Pietschnig:** Writing – review & editing, Visualization, Project administration, Conceptualization.

Declaration of competing interest

The authors declare that they have no known competing financial interests or personal relationships that could have appeared to influence the work reported in this paper.

Data availability

data are available as supporting information.

Acknowledgement

The authors gratefully acknowledge financial support from the Collaborative Research Center “Extreme light for sensing and driving molecular chirality” (CRC 1319 ELCH).

Supplementary materials

Supplementary material associated with this article can be found, in the online version, at doi:10.1016/j.jorganchem.2024.123113.

References

[1] E.J. Fernández, J.M. López-de-Luzuriaga, M. Monge, M.A. Rodríguez, O. Crespo, M. C. Gimeno, A. Laguna, P.G. Jones, Inorg. Chem. 37 (1998) 6002–6006.
[2] X. He, V.W.-W. Yam, Coord. Chem. Rev. 255 (2011) 2111–2123.
[3] V. Fernández-Moreira, R.P. Herrera, M.C. Gimeno, Pure Appl. Chem. 91 (2019) 247–269.
[4] K. Sakakibara, K. Nozaki, Bull. Chem. Soc. Jpn. 82 (2009) 1009–1011.
[5] C.K. Li, X.X. Lu, K.M. Wong, C.L. Chan, N. Zhu, V.W. Yam, Inorg. Chem. 43 (2004) 7421–7430.
[6] E.J. Fernández, J.M. López-de-Luzuriaga, M. Monge, M.A. Rodríguez, O. Crespo, M. C. Gimeno, A. Laguna, P.G. Jones, Chem. - Eur. J. 6 (2000) 636–644.
[7] M. Mosher, P. Kelter, in *An Introduction to Chemistry* (Eds.: M. Mosher, P. Kelter), Springer International Publishing, Cham, 2023, pp. 903–937.
[8] R. Franz, C. Bruhn, R. Pietschnig, Molecules. 26 (2021) 1899.
[9] A.T. Breshears, A.C. Behrle, C.L. Barnes, C.H. Laber, G.A. Baker, J.R. Walensky, Polyhedron. 100 (2015) 333–343.
[10] M. Biosca, M. Coll, F. Lagarde, E. Brémond, L. Routaboul, E. Manoury, O. Pàmies, R. Poli, M. Diéguez, Tetrahedron. (2015) 72.
[11] R. Franz, S. Nasemann, C. Bruhn, Z. Kelemen, R. Pietschnig, Chem. - Eur. J. 27 (2021) 641–648.
[12] D.J. Ager, J. Org. Chem. 49 (1984) 168–170.
[13] N.S. Simpkins, *Ph.D. Dissertation, Imperial College London* 1983.
[14] E.J. Corey, D. Seebach, J. Org. Chem. 31 (1966) 4097–4099.
[15] D.J. Peterson, J. Org. Chem. 33 (1968) 780–784.
[16] D.J. Ager, J. Chem. Soc. Perkin Trans. 1 (1983) 1131–1136.
[17] D.J. Ager, R.C. Cookson, Tetrahedron. Lett. 21 (1980) 1677–1680.
[18] A. Hosomi, M. Hojo, G. Hareau, P. Kocienski, C.R. Smith, Encyclopedia of Reagents for Organic Synthesis (EROS), John Wiley & Sons, Ltd, 2010. Copyright ©.
[19] H.J. Reich, K.J. Kulicke, J. Am. Chem. Soc. 117 (1995) 6621–6622.
[20] P.J. Kocienski, Tetrahedron. Lett. 21 (1980) 1559–1562.
[21] F. Becke, F.W. Heinemann, T. Rüffer, P. Wiegeleben, R. Boese, D. Bläser, D. Steinborn, J. Organomet. Chem. 548 (1997) 205–210.
[22] R. Amsturz, T. Laube, W.B. Schweizer, D. Seebach, J.D. Dunitz, Helv. Chim. Acta 67 (1984) 224–236.
[23] M. Mantina, A.C. Chamberlin, R. Valero, C.J. Cramer, D.G. Truhlar, J. Phys. Chem. A 113 (2009) 5806–5812.
[24] H. Clavier, S.P. Nolan, Chem. Commun. 46 (2010) 841–861.
[25] L. Quin, A. Williams, Practical Interpretation of P-31 NMR Spectra and Computer-Assisted Structure Verification, 2004.
[26] S. Ahmad, A.A. Isab, H.P. Perzanowski, M.S. Hussain, M.N. Akhtar, Transition Met. Chem. 27 (2002) 177–183.
[27] A. Karpus, J.-C. Daran, R. Poli, S. Mazières, M.A. Destarac, E. Manoury, J. Org. Chem. 84 (2019) 9446–9453.
[28] U. Beckmann, D. Süslüyan, P. Kunz, Phosphorus, Sulfur Silicon Relat. Elem. 186 (2011) 1924–1933.
[29] S. Dey, R. Pietschnig, Coord. Chem. Rev. 437 (2021) 213850.
[30] G. Socrates, Infrared and Raman characteristic group frequencies: tables and charts, John Wiley & Sons, Chichester, 2001.
[31] K. Diemert, B. Kottwitz, W. Kuchen, Phosphorus Sulfur Relat. Elem. 26 (1986) 307–320.
[32] M.C. Gimeno, in, Mod. Supramol. Gold Chem. (2008) 1–63.
[33] J. Moussa, L.M. Chamoreau, H. Amouri, RSC. Adv. 4 (2014) 11539–11542.
[34] H. Schmidbaur, A. Schier, Chem. Soc. Rev. 41 (2012) 370–412.
[35] P.G. Chantrell, C.A. Pearce, C.R. Toyer, R. Twaits, J. Appl. Chem. 14 (1964) 563–564.
[36] G. Sheldrick, Acta Cryst. A 64 (2008) 112–122.
[37] O.V. Dolomanov, L.J. Bourhis, R.J. Gildea, J.A.K. Howard, H. Puschmann, J. Appl. Cryst. 42 (2009) 339–341.
[38] C.F. Macrae, P.R. Edgington, P. McCabe, E. Pidcock, G.P. Shields, R. Taylor, M. Towler, J. van de Streek, J. Appl. Cryst. 39 (2006) 453–457.